An approximate method for estimating the stability of geotextile-reinforced embankments

R. K. Rowe and K. L. Soderman
Geotechnical Research Centre, The University of Western Ontario, London, Ont., Canada N6A 5B9

Received January 2, 1985
Accepted April 2, 1985

A method of estimating the short-term stability of reinforced embankments constructed on a deposit that can be idealized as being uniform and purely cohesive is described. This approach maintains the simplicity of conventional limit equilibrium techniques while incorporating the effect of soil–geotextile interaction in terms of an allowable compatible strain for the geotextile. This allowable compatible strain may be deduced from a design chart and depends on the foundation stiffness, the embankment geometry, the depth of the deposit, and the critical height of an unreinforced embankment. The procedure is checked against finite element results and against one published case history.

Key words: embankment, geotextile, analysis, limit equilibrium, finite element, soft clay, shear strength, soil reinforcement.

Dans cet article, on décrit une méthode pour évaluer la stabilité à court terme des remblais armés construits sur un dépôt idéalement constitué d'un matériau uniforme et cohérent. L'approche proposée conserve la simplicité des techniques conventionnelles d'équilibre limite tout en incorporant l'effet de l'inter-action sol–géotextile en terme d'une déformation compatible permissible dans le géotextile. Cette déformation compatible permissible peut être déduite d'une charte de calcul et dépend de la rigidité de la fondation, de la géométrie du remblai, de la profondeur du dépôt et de la hauteur critique d'un remblai non armé. La procédure est vérifiée en partant des résultats d'éléments finis et d'un cas déjà publié.

Mots clés: remblais, géotextile, analyse, équilibre limite, éléments finis, argile molle, résistance au cisaillement, terre armée.

[Traduit par la revue]

Can. Geotech. J. **22**, 392–398 (1985)

Introduction

The stabilizing effect of geotextile reinforcement on embankments has been demonstrated experimentally (e.g. Haliburton *et al.* 1980; Study Centre for Road Construction (SCW) 1981) and theoretically through back analysis of instrumented case histories (e.g. Rowe *et al.* 1984; Rowe and Soderman 1984).

Current approaches to analysis and design of reinforced embankments are based on either limit equilibrium or finite element methods. Although the finite element method has been used successfully in analysis it is recognized that in many practical situations the time and funds may be insufficient to warrant such sophistication. For this reason, extended limit equilibrium techniques are generally preferred because of their simplicity. However, it is the simplifying assumptions of the extended limit equilibrium techniques that hinder their ability to adequately model the complete interaction of the composite geotextile–soil system.

In this paper a method of analysis is presented that maintains the simplicity and versatility of the limit equilibrium techniques and incorporates the essential components of soil–structure interaction derived from the finite element method. The improved method of analysis is incorporated into a practical approach for estimating the stability of reinforced embankments.

Review

Numerous investigators (Bell 1980; Bell *et al.* 1980; Fowler 1982; Haliburton 1981; Ingold 1982; Jewell 1982) have extended limit equilibrium techniques to assess the stability of geotextile-reinforced embankments. The majority of the limit equilibrium techniques are total stress analyses ($\phi = 0$) with assumed circular arc failure surfaces.

Absolute confidence in estimates of embankment stability using limit equilibrium methods is unrealistic (see Milligan and La Rochelle 1984). However, provided the error in the estimate of unreinforced stability is small, successful extension to include the effect of reinforcement is possible (Rowe and Soderman 1984).

In the extended limit equilibrium techniques it is assumed that the reinforcing effect may be modelled as a single restoring force acting at the point of intersection of the free-body boundary and the reinforcement plane. Although the point of application is common in the different approaches, there are various assumptions regarding the direction and magnitude of the restoring force.

Earlier investigators (Bell *et al.* 1980; Fowler 1982; Haliburton 1981) suggested the magnitude of the generated force depends only on the properties of the geotextile. Analyses of this type do not consider the effect of soil–structure interaction on the development of force in the geotextile. Recently, it has been recognized that soil–structure interaction plays an important role in the mobilization of geotextile force and, therefore, its effect cannot be ignored (Jewell 1982; Rowe 1982, 1984; Rowe *et al.* 1984; Rowe and Soderman 1984).

Complete consideration of soil–structure interaction is not possible by limit equilibrium techniques alone. However, further extension of the current limit equilibrium techniques to approximately include interaction effects would prove valuable in design.

Finite element study

The most significant advance of the proposed method of analysis over earlier extended limit equilibrium techniques is the estimation of the allowable geotextile strain by rational means. This method of estimation involves consideration of the effects of soil–structure interaction on the development of geotextile strains prior to embankment collapse as determined from an extensive finite element study.

The finite element analyses were performed with a plane strain nonlinear elastoplastic soil–structure interaction analysis program (LEPSSIA), which is based on the general soil–structure interaction technique proposed by Rowe *et al.* (1978) but

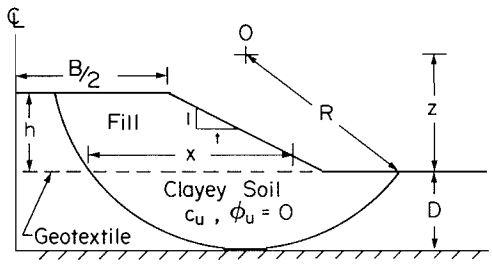

FIG. 1. Cross section of a typical reinforced embankment.

with modifications to take account of the effects of moderate changes in geometry due to deformation of the soil.

The soil was idealized as a nonlinear elastoplastic material with a Mohr–Coulomb failure criterion and a nonassociated flow rule. The geotextile was treated as a structural membrane with an axial stiffness and negligible flexural rigidity. Provision was made for slip between the geotextile and the soil above and (or) below the geotextile. At each point on the interface, the displacement of the soil and geotextile were compatible until the shear stress reached the shear strength defined by a Mohr–Coulomb criterion at the interface. Once the shear strength was reached, slip (i.e., differential tangential displacement between the soil and geotextile) occurred at this location. For each geotextile node, there was a soil node above and a soil node below the geotextile. Thus slip could occur independently above and (or) below the inclusion.

The finite element mesh used in these analyses involved 1472 constant-strain triangular elements. The lateral boundaries were taken to be smooth-rigid and were typically located 66 m from the toe of the embankment. The base was assumed to be rough-rigid but with provision for slip at the base at points where the base-soil shear stress was equal to the shear strength of the soil. Embankment construction was simulated by placing the fill in lifts. Up to five layers were placed in up to 120 load steps.

In analyses performed with geotextile reinforcement, the reinforcement was assumed to be placed on top of the foundation soil over the entire width of the embankment. The soil–geotextile interface shear strength was assumed to be purely cohesive when in contact with the clayey soil and purely frictional on the side in contact with the fill.

A series of finite element analyses was performed on embankments of the type shown in Fig. 1, constructed on a uniform foundation. A variety of soil properties and embankment geometries were analysed (see Tables 1–3). Brittle soils (e.g. quick clay) have not been explicitly considered. The analyses were performed to obtain estimates of collapse loads and geotextile strains for embankments reinforced with geotextiles ranging in "moduli" from 0 to 2000 kN/m. (It should be noted that the axial stiffness of a geotextile is expressed as the force per unit width per unit strain (kN/m) and is commonly referred to as the "modulus" of the geotextile or geogrid.)

Collapse of a reinforced embankment

The collapse height of an unreinforced embankment corresponds to the height at which the shear strength is fully mobilized along a potential rupture surface. However, when dealing with reinforced embankments, collapse involves failure of the soil and, generally, some aspect of the soil–reinforcement system. Clearly, failure of the soil–reinforcement system may take the form of a failure of the soil–geotextile interface (i.e., slip of the geotextile relative to the soil) or a failure of the geotextile. However, if the geotextile permits large deformations prior to reaching failure strain (e.g. low-modulus geotextiles), or if the deposit is deep, then collapse of the reinforced embankment may occur before failure of the geotextile or the geotextile interface. Prior to actual failure of the geotextile or the geotextile–soil interface, the contribution of the geotextile to the embankment stability is governed by a condition of strain compatibility and the relative moduli of the soil and geotextile.

If an embankment is reinforced with a geotextile having a modulus so small that negligible load is developed in the geotextile at collapse, then one would expect the strains just prior to collapse and the collapse height of the reinforced embankment to be the same as those corresponding to failure of a similar unreinforced embankment. The maximum strain that would occur in this geotextile just prior to collapse will be referred to as the "allowable compatible strain."

In the design of reinforced embankments it is considered that failure should be deemed to have occurred if the shear strength of the soil is fully mobilized along a potential rupture surface and (a) the geotextile fails; or (b) the geotextile–soil interface fails; or (c) the maximum strain in the geotextile reaches the "allowable compatible strain."

For high-strength-modulus fabrics the lateral strain in the soil may be significantly reduced by the use of a geotextile and condition (a) or (b) will govern. Condition (c) may be important for lower-modulus fabrics or deep deposits and is intended to limit the strains beneath the reinforced embankment to those which

TABLE 1. Geometry ranges for finite element study

Parameter (see Fig. 1)	Range of values examined
D	3–15 m
B	10–30 m
t	2, 4
D/B	0.11–0.73

TABLE 2. Embankment fill properties for finite element study

Parameter	Value
c'	0
ϕ'	32°
ν'	0.35
E'	$E' = 1000\sigma_3^{0.5}$, where E' = Young's modulus (kPa), σ_3 = minor principal stress (kPa)

TABLE 3. Foundation soil property ranges for finite element study

Parameter	Range of values examined
c_u	3.85–15 kPa
ϕ_u	0°
ν_u	0.48
K_0	0.5
G_s	2.7
e_0	2.5–12.9
γ	11–14.6 kN/m^3
E_u	500–5000 kPa

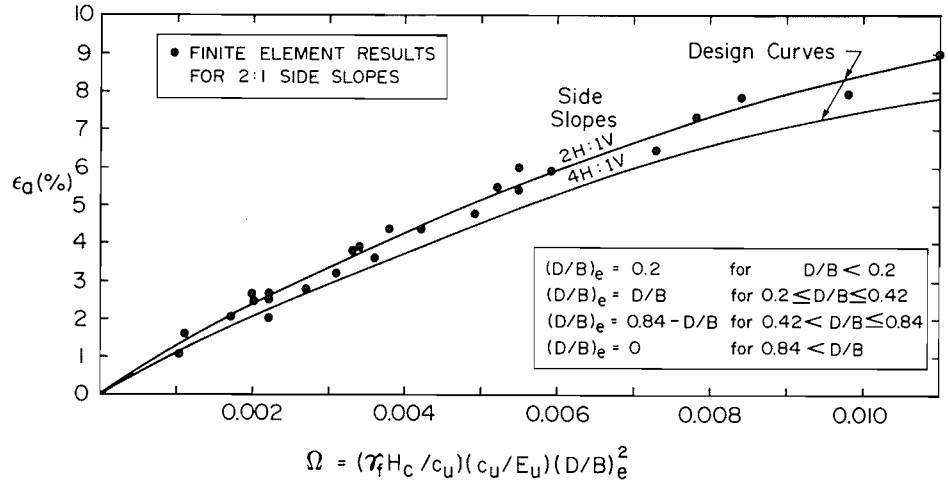

FIG. 2. Allowable compatible strain, ϵ_a, versus dimensionless Ω.

would be obtained just prior to collapse in an unreinforced embankment.

Determination of the allowable compatible strain

An extensive finite element study was performed to determine the allowable compatible strain for a variety of cases. Since the allowable compatible strain is the maximum strain in a geotextile of negligible modulus just prior to collapse, it will depend on the compatible deformations of the soil occurring prior to collapse. These deformations are a function of the width of the embankment B, the depth of the soft soil beneath the embankment D, the undrained modulus of the soil E_u, the undrained shear strength c_u, the unit weight of the fill γ_f, and the height of the embankment at collapse H_c.

It was found that the effect of these parameters could be represented in terms of a single nondimensional parameter Ω defined as

$$[1] \quad \Omega = (\gamma_f H_c/c_u)(c_u/E_u)(D/B)_e^2$$

where γ_f, H_c, E_u, c_u, D, and B are as above and

$$\begin{aligned} &(D/B)_e = 0.2, && D/B < 0.2 \\ &(D/B)_e = D/B, && 0.2 \leq D/B \leq 0.42 \\ &(D/B)_e = 0.84 - D/B, && 0.42 < D/B \leq 0.84 \\ &(D/B)_e = 0, && 0.84 < D/B \end{aligned}$$

$(D/B)_e$ being the effective depth to crest width ratio of the deposit (to be discussed shortly).

The allowable compatible strain may be directly related to the parameter Ω as shown in Fig. 2. It is suggested that in a stability analysis of a reinforced embankment, the force in the fabric T (which contributes to the restoring moment) should not exceed that developed at the allowable compatible strain (i.e., $T \leq \epsilon_a \cdot E_f$ where E_f is the secant modulus of the fabric for the strain range from 0 to ϵ_a).

For a given soil deposit and embankment width B, there is a critical height H_c, which represents the maximum height to which an unreinforced embankment could be constructed. In many cases, the use of geotextile reinforcement will allow construction of the embankment to a height exceeding H_c. However, irrespective of the actual height, it is recommended that the horizontal deformations (and hence the allowable compatible strain ϵ_a) should not be permitted to exceed the values that would be expected just prior to collapse for an unreinforced (or very lightly reinforced) embankment. Thus the allowable strain ϵ_a depends on the critical height H_c and not the actual height of the embankment h.

The effect of a geotextile upon the stability of an embankment depends on the depth D of the deposit relative to the crest width B. For shallow deposits where D/B is less than 0.2, the effective crest width is $B_e = 5D$. That is to say, the failure of the reinforced embankment is controlled by the actual depth of the deposit, and increasing the width of the embankment in excess of B_e will not affect either the collapse height nor the allowable compatible strain (i.e., H_c and ϵ_a for $D/B < 0.2$ will be the same as that for $(D/B)_e = 0.2$).

For values of D/B in the range 0.2–0.42, increasing the D/B ratio increases the strains in the geotextile prior to collapse (all other things being equal) and this may increase the contribution of the geotextile to the embankment stability. However, there is an optimal D/B ratio of approximately 0.42 where the allowable compatible strain is the greatest.

For values of D/B greater than 0.42, increasing D/B actually leads to a reduction in the allowable strain. Figures 3 and 4 show the relative deformations of the soil, at collapse, obtained from finite element analyses for $D/B = 0.33$ and 0.55. An examination of the displacement components at the interface between the embankment and foundation for the two cases reveals that the component of the horizontal displacement is substantially greater for $D/B = 0.33$ than for $D/B = 0.55$. This horizontal displacement is responsible for mobilizing the forces in the geotextile. Thus the inclusion of a geotextile may be expected to have less effect on the stability of an embankment for $D = 0.55B$ than for $D = 0.33B$ (all other things, including B, being constant).

Figure 5 illustrates the variation in the allowable compatible strain with the depth of the deposits for fixed values of B, c_u, E_u, and γ_f (note, however, that H_c does vary with layer depth and is not constant). It can be seen that for this case the peak allowable compatible strain occurs at a depth of approximately 5.7 m ($D/B = 0.42$) and the allowable compatible strain decreases for depths in excess of 5.7 m.

It can be shown that for a deep soil deposit ($D/B > 0.84$) the geotextile has no effect whatsoever on deep-seated stability (although it may still improve local stability near the edge of the embankment). This corresponds to the well-established fact that the bearing capacity of a rough-rigid footing on a deep uniform cohesive layer is identical to that of a smooth-flexible footing

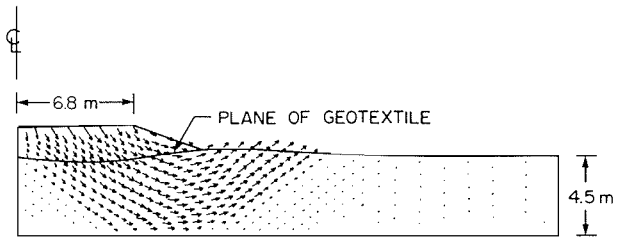

FIG. 3. Velocity field after collapse, $D/B = 0.33$.

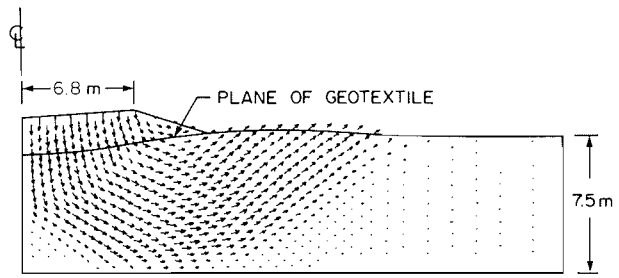

FIG. 4. Velocity field after collapse, $D/B = 0.55$.

(see Hill 1950) and, neglecting the embankment strength, is given by $\gamma_f H_c = 5.14 c_u$.

It was found numerically that the effect of increasing depth, for D/B ratios in the range 0.42–0.84, could be approximately represented by defining Ω in terms of an effective ratio $(D/B)_e$ where

$$(D/B)_e = 0.84 - (D/B)$$

This will give the maximum compatible strain ϵ_a for $D/B = 0.42$ and will give a decrease in Ω (and hence ϵ_a) for $D/B > 0.42$. For $D/B > 0.84$, the allowable strain is zero (i.e. $(D/B)_e = 0$ in [1]).

The relationship between ϵ_a and Ω given in Fig. 2 represents an approximate fit to the finite element results obtained for $B = 13.6$ m and D in the range 3–8.8 m. The actual data points for this case and a 2:1 side slope are shown in the figure. The curve was also checked by performing additional analyses for width B in the range 10–30 m and depth up to 15 m and it was found that the curves given in Fig. 2 provided a very good representation for D/B ratios less than 0.42 and a reasonable envelope (i.e., was conservative) for D/B ratios greater than 0.42.

It has previously been found (e.g. Rowe 1982) that the strains developed in a geotextile depend somewhat on the construction sequence adopted (e.g. an outside–inside construction as compared with construction in horizontal lifts). The curves given in Fig. 2 were checked by performing analyses for alternative construction sequences and it was found that estimates of stability based on allowable strain deduced from Fig. 2 would be conservative in each case. To reduce the likelihood of failure of the fabric due to additional construction-induced strains, the allowable compatible strain should be the minimum of the value deduced from Fig. 2 and 60% of the failure strain of the geotextile where the failure strain is determined from a wide strip test on the particular geotextile.

The magnitude of the strain developed in the geotextile will depend on the deformation of the soil, which, in turn, depends on the undrained modulus of the soil. The effect of the modulus is reflected in the parameter Ω (see eq. [1]) and it can be seen that the lower the modulus, the larger will be Ω and hence (from Fig. 2) the larger will be the allowable compatible strain. Thus,

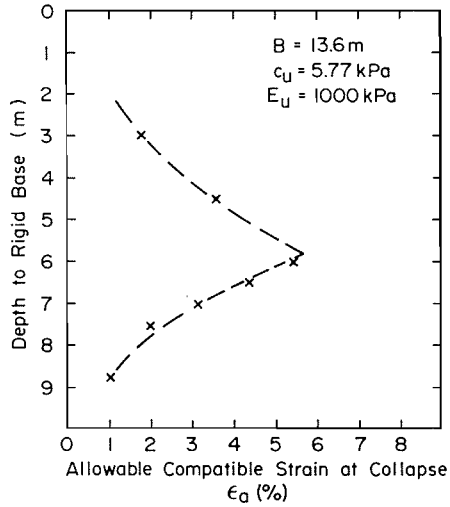

FIG. 5. Effect of depth of deposit on geotextile strains.

it is not conservative to underestimate the undrained modulus of the soil since this would imply larger allowable fabric strains (and a higher fabric force) than may actually be mobilized in the embankment prior to collapse. It should be noted that the ratio E_u/c_u may vary substantially from one soil to another. It may be as low as 125 for soft, highly plastic clays (e.g. see Duncan and Buchignani 1976).

Extended limit equilibrium analysis

The method of analysis proposed here is concerned with the occurrence of rotational slope/foundation failure of a typical reinforced embankment as shown in Fig. 1. The procedure is an extension of the simplified Bishop slip circle analysis (Bishop 1955). Hence the conventional assumptions of the Bishop method apply to the extended approach.

The conventional slip circle method is essentially a method for obtaining an upper bound to the correct collapse load, since it postulates a possible mode of movement without evaluation of a complete stress distribution. When attempting to model a strength increase with depth, errors associated with slip circle analysis can be quite significant *if* a kinematic restraint, such as a strong geotextile, is imposed (Davis and Booker 1975). In this regard, it may be expected that for a soil deposit whose strength increases with depth, the errors associated with the use of slip circle techniques will increase as the effect of the reinforcement increases.

The additional assumptions that are needed in order to include the effect of geotextile reinforcement are the following:

(1) Small strains and undrained response of the foundation.

(2) Any forces due to the geotextile only act to increase the restoring moment; they do not affect the Bishop slice normal forces.

(3) The geotextile force acts at the point of intersection of the geotextile and trial slip circle.

(4) The geotextile is located at, or near, the foundation–fill interface.

(5) Referring to Fig. 1, and defining R = radius of the trial circle and z = vertical distance from the centre of the trial circle to the plane of the geotextile, then the moment arm for calculating the restoring moment due to the geotextile force is taken to be

$$\text{moment arm} = (R + z)/2, \qquad D/B \leq 0.42$$
$$\text{moment arm} = z, \qquad D/B > 0.42$$

(It should be noted that a moment arm of z is conservative for all D/B but may be a little too conservative for $D/B < 0.42$.)

(6) The magnitude of the geotextile force T used to calculate the restoring moment is the lesser of the following: (a) The allowable geotextile force T_a, which is determined from consideration of the ultimate tensile strength of the geotextile and its creep properties. Generally, T_a should not exceed 60% of the ultimate capacity of the geotextile T_u determined from a wide strip tension test at a strain rate of 2%/min. (For some polypropylene- and polyethylene-based geotextile materials a value of $T_a \leq 0.5T_u$ may be necessary.) (b) The maximum bond force T_b that can be developed between the geotextile and the soft foundation. Referring to Fig. 1, this limit is given by $T_b = xc_s$, where x may not exceed half the embankment base width $(B/2 + th)$. (c) The force T_c mobilized in a geotextile of modulus E_f at an allowable compatible strain ϵ_a (i.e. $T_c = \epsilon_a \cdot E_f$). As noted in the last section, the allowable strain will depend on the geometry and soil properties. The effect of these factors may be combined in terms of the dimensionless parameter Ω, where Ω is defined by [1], viz.,

$$\Omega = (\gamma_f H_c/c_u)(c_u/E_u)(D/B)_e^2$$

The relationship between ϵ_a and Ω for a single layer of geotextile is given in Fig. 2 for two different embankment slopes.

(7) The expression for factor of safety has been modified as follows to include the effect of geotextile reinforcement:

$$[2] \quad F = \frac{\Sigma \text{ B.R.M.} + \text{R.R.M.}}{\Sigma \text{ B.O.M.}}$$

where F is the factor of safety for the reinforced embankment; Σ B.R.M. is the sum of the restoring moments (as in the unreinforced case); Σ B.O.M. is the sum of the overturning moments (as in the unreinforced case); and R.R.M. is the restoring moment due to the reinforcement, equal to $T(R + z)/2$ for $D/B \leq 0.42$ and equal to Tz for $D/B > 0.42$. Rearranging the expression for factor of safety yields:

$$[3] \quad \Sigma \text{ B.O.M.} = \frac{\Sigma \text{ B.R.M.} + \text{R.R.M.}}{F}$$

Note the factor of safety F has been applied to both the soil restoring moment and the reinforcement restoring moment. A typical factor of safety is 1.3.

Application

The extended Bishop method of slices, just described, can be incorporated into a simple design procedure. The goal of the procedure is to select geotextile reinforcement that will provide an adequate factor of safety against undrained failure of an embankment on a soil that can be idealized as having a uniform strength. Thus the selection of appropriate reinforcement involves ensuring that there is an adequate factor of safety against collapse due to reinforcement failure, reinforcement creep, reinforcement–soil interface failure, and excessive geotextile strain.

The determination of allowable compatible strains from Fig. 2 is an important aspect of this procedure. Strictly speaking, this figure is only applicable to embankment geometries similar to that in Fig. 1 and the property ranges shown in Tables 1–3. However, with sound engineering judgement this figure may be sufficient for many practical cases.

In this section the proposed design procedure will be presented and its use illustrated by application to typical problems.

Illustrative example 1

This example illustrates how a geotextile reinforcement may be selected to give the desired factor of safety F against rotational failure. The procedure to be adopted involves five steps.

Step 1. Problem definition

Define the required parameters and geometry of the problem as indicated in Fig. 1. Design parameters: (a) geometry: h, D, B, t; (b) fill parameters: c_f, ϕ_f, γ_f; (c) foundation parameters: c_u, E_u, γ; (d) desired factor of safety: F. (Due to the application of the factor of safety, F, to the reinforcing restoring moment (in [3]), the factor of safety associated with the estimation of the mobilized reinforcing force is also F.)

To illustrate the procedure, consider a two-lane highway embankment with parameters $h = 2$ m, $D = 5$ m, $B = 13.5$ m, $t = 2$, $c_f = 0$, $\phi_f = 39°$, $\gamma_f = 21\,\text{kN/m}^3$, $c_u = 8$ kPa, $E_u = 1000$ kPa, $\gamma = 13.5\,\text{kN/m}^3$, and a required factor of safety equal to 1.3.

An iterative procedure is necessary for the determination of the required geotextile properties. As an initial estimate, $E_f = 1000$ kN/m and $T_a = 60$ kN/m have been selected.

Step 2. Determine the collapse height H_c of an unreinforced embankment

(a) Determine F^*, where F^* is the critical factor of safety for an unreinforced embankment of height h (h = design embankment height). If F^* is greater than or equal to F, the required factor of safety, then no reinforcement is required and the procedure is terminated.

(b) Calculate the collapse height H_c.

$$H_c = F^* \cdot h$$

(This calculation is not strictly valid owing to the slight nonlinearity in the relationship between F^* and h; however, a more rigorous examination indicates that the approximation is adequate for most purposes.) For this example, the value of F^* determined for $h = 2$ m is 1.04 and hence $H_c = F^* \cdot h = 2.08$ m.

Step 3. Determine the allowable compatible strain ϵ_a

(a) Calculate

$$\Omega = (\gamma_f H_c/c_u)(c_u/E_u)(D/B)_e^2 = (\gamma_f H_c/E_u)(D/B)_e^2$$

Note that for $D/B \leq 0.2$, $(D/B)_e = 0.2$; for $0.2 < D/B \leq 0.42$, $(D/B)_e = D/B$; for $0.42 < D/B < 0.84$, $(D/B)_e = 0.84 - D/B$; for $0.84 < D/B$, $(D/B)_e = 0$.

(b) With the calculated value of Ω and the given slope parameter t, select the corresponding value of ϵ_a from Fig. 2. For the example: (i) $D/B = 5/13.5 = 0.37$, therefore $(D/B)_e = D/B = 0.37$ and $\Omega = (\gamma_f H_c/E_u)(D/B)^2 = [21(2.08)/1000](5/13.5)^2 = 0.006$. (ii) With $\Omega = 0.006$ and $t = 2$, the value of ϵ_a from Fig. 2 is 5.9%.

Step 4. Determine the factor of safety F_c for the reinforced embankment

Calculate the critical factor of safety F_c for the reinforced embankment of height h, including an additional restoring moment R.R.M., viz.,

$$\begin{aligned} \text{R.R.M.} &= T(R + z)/2, && D/B \leq 0.42 \\ &= Tz, && D/B > 0.42 \end{aligned}$$

where T = minimum of (a) T_a, (b) $T_b = x \cdot c_s$ (see Fig. 1 but where $x \leq (B/2) + th$, (c) $T_c = \epsilon_a \cdot E_f$.

This step requires a computer search for the critical slip circle. The critical circle for the reinforced and unreinforced cases are generally not the same.

For this example, the critical factor of safety is calculated to

be 1.3 and the selection of geotextile forces is governed by the allowable compatible strain of 5.9%. For this case, the interface shear is assumed to be mobilized only along the bottom surface of the geotextile. This conservative assumption is necessary because of the expected differences in the stress–strain behaviour of the top and bottom interfaces.

Step 5. Check the performance of the selected reinforcement

$F_c = F$

If $F_c = F$, the performance of the selected geotextile is satisfactory. If interface slip controls the selection of T (i.e. if T_b is critical), one should reduce the selected geotextile modulus to $E_f \doteq T_b/\epsilon_a$ and repeat steps 4 and 5. This prevents overdesign of the reinforcement. If interface slip does not control the design then the desired geotextile properties (E_f, T_a) have been determined and the solution is complete.

$F_c > F$

If $F_c > F$, select a fabric with a lower E_f and (or) T_a, depending on which property is overdesigned, and repeat steps 4 and 5.

$F_c < F$

If $F_c < F$, select a fabric with a higher E_f and (or) T_a, depending on which property is deficient, and repeat steps 4 and 5. If interface slip governs the selection of T, the desired factor of safety cannot be achieved by inclusion of a single layer of geotextile. A different design is required (e.g. flatter side slopes).

For this example, since the value of $F_c = F = 1.3$ after the first iteration, the performance of the selected reinforcement is adequate and the solution is terminated.

The selected geotextile properties are $E_f = 1000\,\text{kN/m}$ and $T_a = 60\,\text{kN/m}$ for an overall factor of safety of 1.3.

Illustrative example 2

This second example illustrates how the factor of safety F may be determined for a given reinforced embankment. In this case, the procedure involves four steps.

Step 1 is the problem definition. Define the required parameters and geometry of the problem as indicated in Fig. 1. Design parameters: (a) geometry: h, D, B, t; (b) fill parameters: c_f, ϕ_f, γ_f; (c) foundation parameters: c_u, E_u, γ; (d) geotextile parameters: E_f, T_a.

To illustrate the procedure consider the final design arrived at in example 1, including the same design parameters. We are required to estimate the factor of safety F of this embankment against collapse.

Steps 2 through to 4 are carried out identically to example 1.

The factor of safety F is equal to the factor of safety F_c calculated in step 4. (Step 5 is unnecessary.)

For this example, the factor of safety F is 1.3 and the design is governed by the allowable compatible strain.

Comparison of limit equilibrium and finite element results

The proposed extended limit equilibrium method was used to estimate collapse heights for representative cases analysed using the finite element method. A comparison of the collapse heights for reinforced embankments obtained using the limit equilibrium technique with those deduced from finite element analyses indicated excellent agreement, with a maximum discrepancy of less than 4%.

Validation of the extended limit equilibrium approach

The validity of the proposed method of analysis may be assessed in part by a comparison of calculated and observed field behaviour. In this section, consideration will be given to the behaviour of two test embankments constructed in the vicinity of Highway 6 at Almere in the Netherlands. Details regarding the construction and performance of these two embankments are contained in a report by the Study Centre for Road Construction (SCW) (1981) and results of a detailed analysis performed by the authors have been reported by Rowe and Soderman (1984).

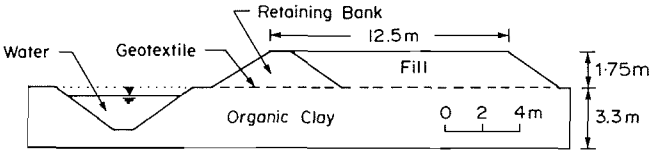

FIG. 6. Typical Almere embankment geometry at unreinforced collapse height.

In October 1979, two sandfill test embankments were constructed on a soft 3–3.5 m thick deposit of organic clay. The clay had an undrained shear strength of about 8 kPa and an undrained modulus of approximately 1000 kPa. One embankment was reinforced with a single layer of geotextile located at the fill–clay interface. The operational modulus of the geotextile was approximately 1900 kN/m. A second embankment, intended as a control section, was constructed without reinforcement. Embankment geometry and geotextile strains were monitored during construction and the approximate geometry of the Almere embankments at the unreinforced collapse height is shown in Fig. 6.

An abrupt collapse of the unreinforced embankment occurred at a nominal height of 1.75 m. This is consistent with a collapse height of 1.72 m calculated by the limit equilibrium method.

Collapse of the reinforced embankment in the field was observed at a nominal height of 2.75 m. The maximum geotextile strain measured at collapse was about 4%.

An analysis of the Almere embankment using the proposed limit equilibrium technique was performed by the authors. In the analysis, the selection of geotextile force mobilized at collapse was governed by an allowable compatible strain of 2.7% as estimated from Fig. 2. The reinforced embankment collapse height was calculated to be 2.55 m.

This conservative estimate of the collapse height is quite encouraging considering that the estimate of allowable compatible strain did not take into account the effect of the ditch excavated at the toe of the embankment as indicated in Fig. 6 (although the ditch was considered in the limit equilibrium analysis).

Conclusion

A method of estimating the short-term stability of reinforced embankments constructed on a uniform purely cohesive foundation has been described. This approach maintains the simplicity of simple limit equilibrium techniques while incorporating the effects of soil–geotextile interaction in terms of an allowable compatible strain for the geotextile. This allowable compatible strain may be deduced from a design chart and depends on the foundation stiffness, the embankment geometry, the deposit depth, the unit weight of the fill, and the critical height of an unreinforced embankment. The procedure has been checked against finite element results and against one published case history. On the basis of the encouraging agreement, it is suggested that further testing of the proposed technique is warranted.

Acknowledgements

The work described in this paper is part of a study directed at developing improved design procedures for geotextile-reinforced embankments. This study is primarily funded by the Ontario Ministry of Transportation and Communications. Additional funding was supplied by The Natural Sciences and Engineering Research Council of Canada under Grant A-1007. The authors are grateful to Messrs. V. Milligan and M. D. MacLean for their useful comments on the manuscript.

BELL, J. R. 1980. Design criteria for selected geotextile installations. First Canadian Symposium on Geotextiles, Calgary, Alta., pp. 35–57.

BELL, J. R., HICKS, R. G., COPELAND, S., EVANS, G. L., CONGRE, J. J., and MALLORD, P. 1980. Evaluation of test methods and use criteria for geotechnical fabrics in highway applications. U.S. Dept. of Transportation, F.H.A., Washington, DC, Interim Report to FHWA/RD-80/021.

BISHOP, A. W. 1955. The use of slip circle in the stability analysis of slopes. Proceedings of the European Conference on Stability of Earth Slopes, Vol. 1, pp. 1–13; see also Geotechnique, **5**, pp. 7–17.

DAVIS, E. H., and BOOKER, J. R. 1975. Application of plasticity theory to foundations. *In* Soil mechanics—recent developments. *Edited by* S. Valliapan, S. Hain, and I. K. Lee. Butterworths, Sydney, N.S.W., Australia, Chapt. 3, pp. 83–112.

DUNCAN, J. M., and BUCHIGNANI, A. L. 1976. An engineering manual for settlement studies. Geotechnical report, Department of Civil Engineering, University of California at Berkeley, Berkeley, CA. 94 p.

FOWLER, J. 1982. Theoretical design considerations for fabric reinforced embankments. Proceedings of the 2nd International Conference on Goetextiles, Las Vegas, NV, Vol. 2, pp. 665–670.

HALIBURTON, T. A. 1981. Use of engineering fabric in road and embankment construction. Seminar on the Use of Synthetic Fabrics in Civil Engineering, Toronto, Ont., pp. 66–94.

HALIBURTON, T. A., FOWLER, J., and LANGAN, J. P. 1980. Design and construction of fabric-reinforced embankment test section at Pinto Pass, Mobile, Alabama. Transportation Research Record, No. 749, pp. 27–33.

HILL, R. 1950. Mathematical theory of plasticity. Oxford University Press, London, England.

INGOLD, T. S. 1982. An analytical study of geotextile reinforced embankments. Proceedings of the 2nd International Conference on Geotextiles, Las Vegas, NV, Vol. 2, pp. 683–688.

JEWELL, R. A. 1982. A limit equilibrium design method for reinforced embankments on soft foundations. Proceedings of the 2nd International Conference on Geotextiles, Las Vegas, NV, Vol. 2, pp. 671–676.

MILLIGAN, V., and LA ROCHELLE, P. 1984. Design methods for embankments over weak soils. Symposium on Polymer Grid Reinforcement in Civil Engineering, Institute of Civil Engineers, London, U.K., Paper No. 3.4.

ROWE, R. K. 1982. The analysis of an embankment constructed on a geotextile. Proceedings of the 2nd International Conference on Geotextiles, Las Vegas, NV, Vol. 2, pp. 677–682.

——— 1984. Reinforced embankments: analysis and design. ASCE Journal of the Geotechnical Engineering Division, **110**(GT2), pp. 231–246.

ROWE, R. K., and SODERMAN, K. L. 1984. Comparison of predicted and observed behaviour of two test embankments. International Journal of Geotextiles and Geomembranes, **1**(1), pp. 157–174.

ROWE, R. K., BOOKER, J. R., and BALAAM, N. P. 1978. Application of the initial stress method to soil–structure interaction. International Journal for Numerical Methods in Engineering, **12**(5), pp. 873–880.

ROWE, R. K., MACLEAN, M. D., and SODERMAN, K. L. 1984. Analysis of a geotextile-reinforced embankment constructed on peat. Canadian Geotechnical Journal, **21**(3), pp. 563–576.

STUDY CENTRE FOR ROAD CONSTRUCTION (SCW). 1981. Stability of slopes constructed with polyester reinforcing fabric. Arnhem, The Netherlands.

List of symbols

B	embankment crest width
c_f	cohesion intercept for the embankment fill
c_s	geotextile–soil interface cohesion
c_u	undrained shear strength of the foundation soil
D	depth of the foundation soil
ϵ_a	allowable compatible geotextile strain
E_f	geotextile "modulus" in kN/m
e_0	initial void ratio of the foundation soil
E_u	undrained modulus of the foundation soil
F	factor of safety against embankment failure
G_s	specific gravity of solids for foundation soil
γ	unit weight of the foundation soil
γ_f	unit weight of the embankment fill
h	embankment height
H_c	collapse height of an unreinforced embankment
K_0	coefficient of lateral earth pressure at rest in foundation
ϕ_u	undrained angle of internal friction for the foundation soil
ϕ_f	angle of internal friction for the embankment fill
R	radius of trial slip circle
t	embankment slope parameter
T_a	allowable tensile capacity of the geotextile in kN/m
T_b	allowable geotextile force in kN/m due to geotextile–soil bond
T_c	geotextile force in kN/m due to the allowable compatible strain
T	geotextile force in kN/m mobilized at collapse
ν_u	Poisson's ratio of the foundation soil
x	geotextile–soil interface slip length
z	vertical distance from the centre of the trial slip circle to the geotextile